ELSEVIER

International Journal of Mass Spectrometry 195/196 (2000) 149–170

International Journal of Mass Spectrometry

Activation of CH_4, C_2H_6, and C_3H_8 by gas-phase Nb^+ and the thermochemistry of Nb–ligand complexes

M.R. Sievers, Y.-M. Chen, C.L. Haynes, P.B. Armentrout*

Department of Chemistry, University of Utah, Salt Lake City, UT 84112, USA

Received 7 June 1999; accepted 10 August 1999

Abstract

The kinetic energy dependence of the reactions of Nb^+ (^5D) with methane, ethane, and propane have been studied using guided ion beam mass spectrometry. It is found that dehydrogenation is efficient and the dominant process at low energies in all three reaction systems. At high energies, products resulting from both C–H and C–C cleavage processes are appreciable. The observation of dihydride and hydrido-methyl niobium cation products provides insight into the reaction mechanisms operating in these processes. The results for Nb^+ are compared with those for the first-row transition metal congener V^+ and the differences in behavior and mechanism discussed. Modeling of the endothermic reaction cross sections yields the 0 K bond dissociation energies (in electron volts) of D_0(Nb–H) $>$ 2.3 ± 0.1, $D_0(Nb^+–2H)$ = 4.64 ± 0.06, $D_0(Nb^+–C)$ = 5.28 ± 0.15, $D_0(Nb^+–CH)$ = 6.02 ± 0.20, $D_0(Nb^+–CH_2)$ = 4.44 ± 0.09, $D_0(Nb^+–CH_3)$ = 2.06 ± 0.11, $D_0[Nb^+–(H)(CH_3)]$ = 4.78 ± 0.11, $D_0(Nb^+–C_2H)$ = 4.34 ± 0.19, $D_0(Nb^+–C_2H_2)$ = 2.90 ± 0.06, $D_0(Nb^+–C_2H_3)$ = 3.43 ± 0.21, $D_0(Nb^+–C_2H_4)$ = 2.8 ± 0.3, $D_0(Nb^+–C_2H_5)$ = 2.45 ± 0.12, $D_0(Nb^+–C_3H_2)$ = 5.25 ± 0.19, and lower limits for $D_0(Nb^+–C_3H_3)$ ≥ 3.76 ± 0.23 and $D_0(Nb^+–C_3H_5)$ ≥ 1.4 ± 0.1. The observation of exothermic processes sets lower limits for the bond energies of Nb^+ to propyne and propene of 2.84 and 1.22 eV, respectively. (Int J Mass Spectrom 195/196 (2000) 149–170) © 2000 Elsevier Science B.V.

Keywords: Bond activation; Thermochemistry; Niobium; Transition metal ions; Bond energies

1. Introduction

A long term goal of research in our laboratory has been the study of the reactions of transition metal ions (M^+) with small hydrocarbons. Studies of such systems for first-row transition metal elements is extensive [1–10]. Such studies can reveal the electronic requirements for the activation of C–H and C–C bonds at metal centers [2–5] and provide an examination of the periodic trends in such reactivity unavailable in condensed phase media [1,2]. A particular strength of the guided ion beam methods used in our laboratory is the derivation of metal-hydrogen and metal–carbon bond dissociation energies (BDEs) [6–10]. Such thermochemistry is of obvious fundamental interest and also has implications in understanding a variety of catalytic reactions involving transition metal systems [11]. Studies of the reactivity of second-row transition metal cations are also abundant [12–24], but somewhat less systematic and extensive [25]. In our laboratory, we have studied the activation of several small hydrocarbons by the sec-

* Corresponding author. E-mail: armentrout@chemistry.utah.edu

Dedicated to the memory of Robert R. Squires and in thanks for his contributions to ion chemistry.

PII S1387-3806(99)00170-0

ond-row transition metal ions: Y^+ [26], Ru^+ [27], Rh^+ [28,29], Pd^+ [30], and Ag^+ [31].

In the present study, we extend this work to examine Nb^+ and describe its reactions with methane, ethane, and propane. These systems have been examined at thermal energies by Freiser and co-workers [14,15] using ion cyclotron resonance (ICR) mass spectrometry. Consequently, only exothermic processes were examined. Dehydrogenation (and in some cases, double and triple dehydrogenation) were found to be the major reactions for all hydrocarbon systems examined (cyclic and acyclic). Here, we are able to investigate the reactions of Nb^+ with the three smallest saturated hydrocarbons over a wide range of kinetic energies, examining both endothermic and exothermic processes. This permits the extraction of systematic thermodynamic as well as mechanistic information.

There is relatively little thermochemistry available for niobium species in the literature, as shown in Table 1. We have previously measured BDEs for Nb^+–H, Nb^+–C, and Nb^+–O by determining the endothermicities of the formation of these species from reactions of Nb^+ with H_2 (and D_2) [32] and CO [33]. Hettich and Frieser examined the photodissociation of $NbCH_2^+$ and observed Nb^+, NbC^+, and $NbCH^+$ products [34]. From the thresholds for these dissociations, they determined the bond energies of Nb^+–C, Nb^+–CH, and Nb^+–CH_2 listed in Table 1. Photodissociation was also used by Ranatunga and Freiser to measure the Nb^+–C_2H_2 bond energy [35]. Bowers has measured the binding energies of 1–8 H_2 molecules to Nb^+ using equilibrium methods [36]. In addition, theoretical calculations have been performed for the BDEs of several species relevant to the present work: NbH^+ [37–40], NbH [41,42,43], $Nb(H)_2^+$ [44], $NbCH_2^+$ [40,45], $NbCH_3^+$ [43], $Nb(H)(CH_3)^+$ and $Nb(CH_4)^+$ [23], $Nb(CH_3)_2^+$ and $Nb(C_2H_6)^+$ [46], and $Nb(C_2H_2)^+$ [47].

As can be seen from Table 1, the previously measured BDEs generally have large uncertainties and are determined by only a single technique, except in the NbC^+ case. Good agreement between experiment and theory is found for NbH^+ and $Nb(C_2H_2)^+$, whereas there is a large discrepancy for $NbCH_2^+$. In the present work, we measure several new BDEs by determining the endothermic reaction thresholds for reactions of Nb^+ with the three hydrocarbons. We use a dc-discharge flow tube ion source to produce Nb^+ ions that are believed to be in the ^5D electronic ground state term [32]. Thus, the threshold measurements have few complexities associated with the presence of excited state ions.

One of the challenging problems in the study of alkane activation by transition metal ions is to determine reaction mechanisms. Detailed experimental [48–52] and theoretical [53–57] studies of first-row transition metal cations (mostly Fe^+, Co^+, and Ni^+) have been carried out to elucidate the mechanisms, whereas many fewer studies that emphasize mechanisms for second-row transition metal cations have been performed [23,28,29,53]. Nevertheless, it is clear that the mechanisms do vary, both from early to late and from first-row to second-row transition metal cations, as we have recently reviewed [25]. Here, we examine the likely mechanisms for reactions of Nb^+ and compare them to those for the first-row congener, V^+ [50,58–64].

2. Experimental

2.1. General

These studies are performed using a guided ion beam tandem mass spectrometer. The instrument and experimental methods have been described previously [65,66]. Ions, formed as described in the following, are extracted from the source, accelerated, and focused into a magnetic sector momentum analyzer for mass analysis. The ions are decelerated to a desired kinetic energy and focused into an octopole ion guide that radially traps the ions. While in the octopole, the ions pass through a gas cell that contains the neutral reactant at pressures where multiple collisions are improbable ($<$0.30 mTorr). Single collision conditions were verified by examining the pressure dependence of the cross sections measured here. The product ions and the reactant ion beam drift out of the gas cell, are focused into a quadrupole mass filter and

Table 1
Nb^+–L bond energies (eV) at 0 K (values marked with an asterisk refer to dissociation to the indicated products from an electrostatic complex, $Nb(H_2)^+$, $Nb(CH_4)^+$, or $Nb(C_2H_6)^+$, rather than from the covalently bound species indicated)

		Previous work	
Species	This work	Experiment	Theory
Nb^+–H		2.28 (0.07)[a]	2.11,[b] 2.28 (0.13),[c] 2.34,[d] 2.45[e]
Nb–H	>2.3 (0.1)		2.55,[f] 2.56[g]
Nb^+–2H	4.64 (0.06)	5.15 (0.04)[h]*	4.14[i]
Nb^+–O		7.13 (0.11)[j]	
Nb^+–C	5.28 (0.15)	5.16 (0.15),[j] >5.7[k]	
Nb^+–CH	6.02 (0.20)	6.29 (0.35)[k]	
Nb^+–CH_2	4.44 (0.09)	4.60 (0.30)[k]	4.12,[e] 3.86 (0.13)[l]
Nb^+–CH_3	2.06 (0.11)		2.15 (0.13)[f]
Nb–CH_3			2.20[f]
Nb^+–(H)(CH_3)	4.78 (0.11)		5.06,[m] 5.26[m]*
Nb^+–2CH_3			4.47,[n] 4.25[n]*
Nb^+–C_2H	4.34 (0.19)		
Nb^+–C_2H_2	2.90 (0.06)	2.47 (0.13)[o]	2.56 (0.13)[p]
Nb^+–C_2H_3	3.43 (0.21)		
Nb^+–C_2H_4	2.8 (0.3)		
Nb^+–C_2H_5	2.45 (0.12)		
Nb^+–C_3H_2	5.25 (0.19)		
Nb^+–C_3H_3	≥3.76 (0.23)		
Nb^+–C_3H_4	>2.84		
Nb^+–C_3H_5	>1.39 (0.08)		
Nb^+–C_3H_6	>1.22		

[a] [32].
[b] [37].
[c] [38].
[e] [39].
[e] [40].
[f] [43].
[g] [42].
[h] [35].
[i] [44].
[j] [33].
[k] [34].
[l] [45].
[m] [23].
[n] [46] and [10].
[o] [35].
[p] [47].

then detected by a secondary electron scintillation detector. Ion intensities are converted to absolute cross sections as described previously [65]. Uncertainties in the absolute cross sections are estimated at ±20%.

To determine the absolute zero and distribution of the ion kinetic energy, the octopole is used as a retarding energy analyzer [65]. The uncertainty in the absolute energy scale is ±0.05 eV (lab). The full width at half maximum of the ion energy distribution is 0.2–0.4 eV (lab). Lab energies are converted into center-of-mass energies using $E(\mathrm{CM}) = E(\mathrm{lab})\, m/(m + M)$ where M and m are the masses of the ion and neutral reactant, respectively. At the lowest energies, the ion energies are corrected for truncation of the ion beam as described previously [65]. All energies in the following text are in the center-of-mass frame.

2.2. Ion source

The ion source used here is a dc discharge/flow tube (DC/FT) source described in previous work [66]. The DC/FT source utilizes a niobium cathode held at 1.5–3 kV over which a flow of approximately 90% He and 10% Ar passes at a typical pressure of ~0.5 Torr. Ar^+ ions created in a direct current discharge are accelerated toward the niobium cathode, sputtering off atomic metal ions. The ions then undergo ~10^5 collisions with He and ~10^4 collisions with Ar in the meter long flow tube before entering the guided ion

beam apparatus. Results obtained previously [32] indicate that the ions produced in the DC/FT source are exclusively in their $a\ ^5D$ ground state. This study determined that the electronic temperature is below 900 K and likely to be at 300 ± 100 K.

2.3. Data analysis

Previous theoretical [58,67] and experimental work [68] has shown that endothermic cross sections can be modeled by using

$$\sigma(E) = \sigma_0 \sum g_i(E + E_{el} + E_i - E_0)''/E \quad (1)$$

where σ_0 is an energy independent scaling parameter, E is the relative translational energy of the reactants, E_{el} is the average electronic energy of the Nb^+ reactant, E_0 is the reaction threshold at 0 K, and n is a parameter that controls the shape of the cross section. The summation is over each rovibrational state of the reactants having relative populations g_i and energies E_i. The various sets of vibrational frequencies used in this work are taken from the literature [69].

Before comparison with the data, the model is convoluted over the neutral and ion kinetic energy distributions using previously developed methods [65]. The parameters E_0, σ_0, and n are then optimized using a nonlinear least squares analysis in order to best reproduce the data. Reported values of E_0, σ_0, and n are mean values for each parameter from the best fits to several independent sets of data and uncertainties are one standard deviation from the mean. The listed uncertainties in the E_0 values also include the uncertainty in the absolute energy scale and the uncertainty in the electronic energy of Nb^+.

3. Results

Cross sections for reaction of Nb^+ with the three small alkanes are presented in the following sections. In some cases, these cross sections have been corrected for mass overlap between products ions having adjacent masses. Thermodynamic information for the stable and radical hydrocarbons required to interpret these results has recently been compiled [30]. The only additional values needed here are those for C_2H and C_3H_2, which have heats of formation at 0 K of 5.82 ± 0.03 [70] and 5.61 ± 0.17 eV [71].

3.1. $Nb^+ + CH_4$

Reaction of Nb^+ with methane yields the products indicated in

$$Nb^+ + CH_4 \rightarrow NbH^+ + CH_3 \quad (2)$$

$$\rightarrow NbC^+ + 2H_2 \quad (3)$$

$$\rightarrow NbCH^+ + H_2 + H \quad (4)$$

$$\rightarrow NbCH_2^+ + H_2 \quad (5)$$

$$\rightarrow NbCH_3^+ + H \quad (6)$$

Fig. 1 shows the analogous results for perdeuterated methane, which enhances the mass resolution, thereby allowing the products of reactions (3)–(6) to be more easily separated. Results for CH_4 and CD_4 are very similar.

The lowest energy pathway is dehydrogenation of methane to form $NbCH_2^+$, reaction (5). The cross section rises from an apparent threshold near zero and continues to rise until near 0.7 eV where it starts to slowly fall off. Near 2.6 eV, the $NbCH_2^+$ cross section declines more rapidly, which could be a result of decomposition or competition with another product. $NbCH_2^+$ can decompose by losing CH_2 to form Nb^+ starting at 4.71 eV = $D_0(H_2–CH_2)$, by dehydrogenation to form NbC^+, or to lose an H atom to form $NbCH^+$. Clearly the former channel begins too high in energy to account for the decline and the NbC^+ channel is too small to account for all of the decline. Although the $NbCH^+$ channel has sufficient intensity, it starts too high in energy (which can be seen by examining the sum of the $NbCH_2^+$ and $NbCH^+$ cross sections). Instead, we find that the increase in the NbH^+ cross section exactly compensates for the decline observed in the $NbCH_2^+$ cross section, indicating that this decline is primarily a result of depletion of a common intermediate by production of NbH^+, as discussed below.

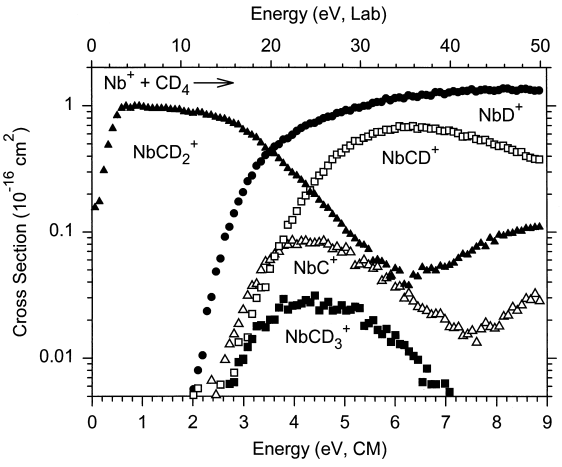

Fig. 1. Cross sections for reactions of Nb^+ with CD_4 as a function of kinetic energy in the center-of-mass frame (lower axis) and laboratory frame (upper axis).

The NbH^+ cross section rises from an apparent threshold near 2 eV and continues rising until ~5 eV where it levels off. The other primary product formed in this system is $NbCH_3^+$, formed in reaction (6). The cross section for this product is small, apparently the result of competition with the nearly isoenergetic reaction (2) and rapid dehydrogenation to form $NbCH^+$. This sequence is more evident in the reactions of Nb^+ with the larger alkanes. An alternate decomposition pathway is H atom loss to form $NbCH_2^+$, which is evident as the rise in the $NbCH_2^+$ cross section beginning about 6 eV. The $NbCH^+$ and NbC^+ cross sections begin to rise near 2.5 eV. As previously noted, the $NbCH^+$ species comes from dehydrogenation of the primary $NbCH_3^+$ product. The NbC^+ product must result from dehydrogenation of the primary $NbCH_2^+$ product. The secondary feature in this cross section starting at about 7.5 eV mimics the secondary rise in the $NbCH_2^+$ cross section, delayed by the energetics for dehydrogenation.

In previous investigations of this reaction at thermal energies, Buckner and Freiser [15] first reported observation of reaction (5) with an efficiency of 0.008, which corresponds to a cross section at our lowest energies of 1×10^{-16} cm^2. Later, Buckner et al. [14] concluded that Nb^+ was unreactive with CH_4 when the ion was properly cooled to eliminate excited electronic states. This is consistent with the present observations as the small amount of reactivity that we observe at thermal energies (a reaction efficiency of ~0.0015) would be too small to observe routinely by ICR. Freiser and co-workers [14,34] also report that the reverse of reaction (5) occurs readily, indicating that there is no barrier in excess of the endothermicity for reaction (5). These authors also found that collisional [14] or photoexcitation [34] of the $NbCH_2^+$ product leads to dissociation by H atom loss, H_2 loss, and CH_2 loss. This is consistent with the decomposition pathways noted here.

3.2. $Nb^+ + C_2H_6$

The reaction of niobium cation with ethane yields the products listed in the following [these are shown in Fig. 2(a) and (b)]:

$$Nb^+ + C_2H_6 \rightarrow NbH^+ + C_2H_5 \quad (7)$$

$$\rightarrow NbH_2^+ + C_2H_4 \quad (8)$$

$$\rightarrow NbC^+ + CH_2 + 2\,H_2 \quad (9)$$

$$\rightarrow NbCH^+ + CH_3 + H_2 \quad (10)$$

$$\rightarrow NbCH_2^+ + CH_4 \quad (11)$$

$$\rightarrow NbCH_3^+ + CH_3 \quad (12)$$

$$\rightarrow NbC_2H^+ + 2H_2 + H \quad (13)$$

$$\rightarrow NbC_2H_2^+ + 2H_2 \quad (14)$$

$$\rightarrow NbC_2H_3^+ + H_2 + H \quad (15)$$

$$\rightarrow NbC_2H_4^+ + H_2 \quad (16)$$

Fig. 2(a) shows all product channels in which the C–C bond is retained. The dominant reaction of Nb^+ with ethane at low energies is dehydrogenation, reaction (16). The cross section for this process declines with increasing energy, consistent with a exothermic reaction having no barriers in excess of the energy of the reactants. This cross section declines as $E^{-0.5}$ from 0 to 0.2 eV, consistent with the Langevin-Gioumousis-Stevenson (LGS) collision cross section for ion–molecule collisions [72]. The magnitude of this cross

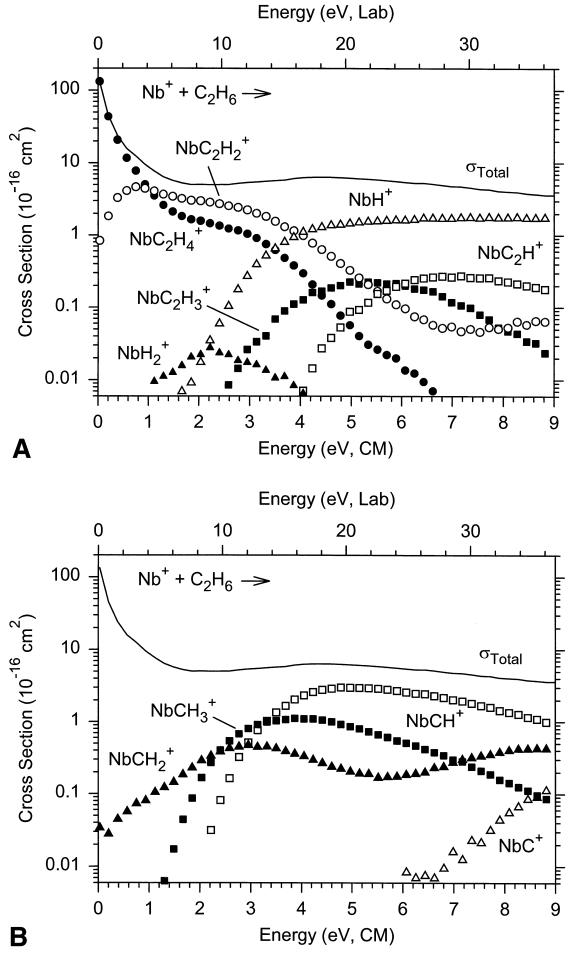

Fig. 2. Cross sections for reactions of Nb^+ with C_2H_6 as a function of kinetic energy in the center-of-mass frame (lower axis) and laboratory frame (upper axis). (a) Results for C–H bond cleavage reactions and (b) for C–C bond cleavage reactions. The full lines in (a) and (b) show the total reaction cross section for both parts.

section at thermal energies (0.04 eV) is 66% of the LGS cross section. Above 0.2 eV, the $NbC_2H_4^+$ cross section drops more rapidly ($\sim E^{-1.7}$) as the $NbC_2H_2^+$ product is formed. This indicates that the slightly endothermic double dehydrogenation, reaction (14), depletes the $NbC_2H_4^+$ product. The total cross section declines as $E^{-1.0}$ from 0.2 to 1.8 eV. Above about 2.5 eV, both the $NbC_2H_4^+$ and $NbC_2H_2^+$ product cross sections begin to decline much more rapidly. This is apparently caused by competition with the formation of NbH^+ in reaction (7) as no other product has a cross section of sufficient intensity to account for the declines. The sum of the $NbC_2H_4^+$, $NbC_2H_2^+$, and NbH^+ cross sections decreases smoothly, thereby indicating that the latter channel is likely to deplete a common intermediate, as discussed below.

At higher energies, $NbC_2H_3^+$ is formed in reaction (15). This species must come either from H atom loss from the $NbC_2H_4^+$ product or could evolve from dehydrogenation of $NbC_2H_5^+$. Although this latter product was looked for and not observed, it is possible that the $NbC_2H_5^+$ species loses H_2 readily such that its cross section never reaches an appreciable magnitude. This hypothesis is consistent with the relative magnitudes of the $NbC_2H_5^+$ and $NbC_2H_3^+$ cross sections observed in the propane system (see below). The cross section for $NbC_2H_3^+$ rises from an apparent threshold near 2.5 eV until near 5 eV where it begins to fall off. This decline is largely attributable to further dehydrogenation to form NbC_2H^+ in reaction (13). A competing dissociation pathway is H atom loss to form $NbC_2H_2^+$, which can be seen as the rise in this cross section starting near 7 eV.

One interesting minor product observed is NbH_2^+, formed in reaction (8). This process competes directly with dehydrogenation to form $NbC_2H_4^+$ in reaction (16). Clearly endothermic, this reaction reaches a maximum cross section very close to the threshold observed for NbH^+ formation. The NbH_2^+ cross section does not reach a maximum at this energy because this species decomposes to NbH^+, as this process corresponds to the overall formation of $NbH^+ + H + C_2H_4$, which cannot occur until 3.54 ± 0.07 eV. Therefore, the NbH_2^+ cross section must decline at this energy because the NbH^+ channel depletes a common intermediate.

Fig. 2(b) shows the products formed by cleavage of the C–C bond in ethane. The lowest energy product is the formation of $NbCH_2^+$, indicating the neutral product must be methane, reaction (11). This product cross section rises slowly from an apparent threshold near 0 eV, characteristic of an inefficient near-thermoneutral reaction. The cross section rises until near 3 eV then declines before rising again near 5.5 eV. This latter feature must correspond to $CH_3 + H$ products, which can begin at $D_0(CH_3–H) = 4.55$ eV above the thresh-

old for reaction (11). The $NbCH_3^+$ cross section rises from an apparent threshold near 1.5 eV, continues rising to near 4 eV, and then falls off. The shape of the cross section indicates that $NbCH_3^+$ loses H_2 to form $NbCH^+$. A minor decomposition channel is also H atom loss to form $NbCH_2^+$, accounting for the high energy feature in the $NbCH_2^+$ cross section. The $NbCH^+$ cross section rises from an apparent threshold near 2 eV and reaches a maximum near 4.5 eV, which we attribute to decomposition of the $NbCH_3^+$ precursor to $Nb^+ + CH_3$, a process that can begin at $D_0(CH_3–CH_3) = 3.90$ eV. At very high energies, NbC^+ is also observed and is attributable to reaction (9). This can occur by H atom loss from $NbCH^+$ or possibly by H_2 loss from $NbCH_2^+$. It seems likely that NbC^+ is also formed at lower energies along with $CH_4 + H_2$ neutral products, but the cross section for such a reaction is obscured by mass overlap with the much more intense $NbCH^+$ product in this energy region.

In previous work on this system at thermal energies, Buckner et al. [14] observed the dehydrogenation and double dehydrogenation processes, reactions (16) and (14), with a branching ratio of 58:42. No reaction efficiency was reported. Such a branching ratio is observed in our work [Fig. 2(a)] at a kinetic energy of about 0.8 eV, suggesting that the ICR study has kinetically excited ions or possibly that the electronically excited states of Nb^+ are not cooled as completely as believed. Similar conclusions have been drawn [29] in comparing our results for similar reactions of Rh^+ with those from Freiser and coworkers. Buckner et al. also examined the $Nb(C_2H_4)^+$ and $Nb(C_2H_2)^+$ products by subsequent collision-induced dissociation. The former product dehydrogenated further and lost C_2H_4, whereas the latter product lost only the C_2H_2 ligand. This indicates that the ligands are ethene and ethyne.

3.3. $Nb^+ + C_3H_8$

The reaction of niobium cation with propane yields a plethora of products as formed in

$$Nb^+ + C_3H_8 \rightarrow NbH^+ + C_3H_7 \quad (17)$$

$$\rightarrow NbH_2^+ + C_3H_6 \quad (18)$$

$$\rightarrow NbC^+ + C_2H_4 + 2\,H_2 \quad (19)$$

$$\rightarrow NbCH^+ + C_2H_5 + H_2 \quad (20)$$

$$\rightarrow NbCH_2^+ + C_2H_6 \quad (21)$$

$$\rightarrow NbCH_3^+ + C_2H_5 \quad (22)$$

$$\rightarrow NbCH_4^+ + C_2H_4 \quad (23)$$

$$\rightarrow NbC_2H^+ + CH_3 + 2H_2 \quad (24)$$

$$\rightarrow NbC_2H_2^+ + CH_4 + H_2 \quad (25)$$

$$\rightarrow NbC_2H_3^+ + CH_3 + H_2 \quad (26)$$

$$\rightarrow NbC_2H_4^+ + CH_4 \quad (27)$$

$$\rightarrow NbC_2H_5^+ + CH_3 \quad (28)$$

$$\rightarrow NbC_3H_2^+ + 3H_2 \quad (29)$$

$$\rightarrow NbC_3H_3^+ + 2H_2 + H \quad (30)$$

$$\rightarrow NbC_3H_4^+ + 2H_2 \quad (31)$$

$$\rightarrow NbC_3H_5^+ + H_2 + H \quad (32)$$

$$\rightarrow NbC_3H_6^+ + H_2 \quad (33)$$

$$\rightarrow C_2H_3^+ + NbH + CH_4 \quad (34)$$

$$\rightarrow C_3H_5^+ + NbH + H_2 \quad (35)$$

$$\rightarrow C_3H_7^+ + NbH \quad (36)$$

These cross sections are shown in Fig. 3. The total cross section declines as $E^{-0.5}$ from 0 to 0.6 eV and has a magnitude of 1.2×10^{-14} cm^2 at 0.04 eV. Both the energy dependence and the magnitude are consistent with the LGS collision cross section for ion–molecule collisions [72]. This region of the total cross section can be reproduced by scaling the LGS cross section by 0.94.

The dominant products observed involve the loss of hydrogen from the transient $NbC_3H_8^+$ intermediate to form $NbC_3H_x^+$ products as shown in Fig. 3(a). The primary product in this sequence is $NbC_3H_6^+$ formed by dehydrogenation of propane in reaction (33). This

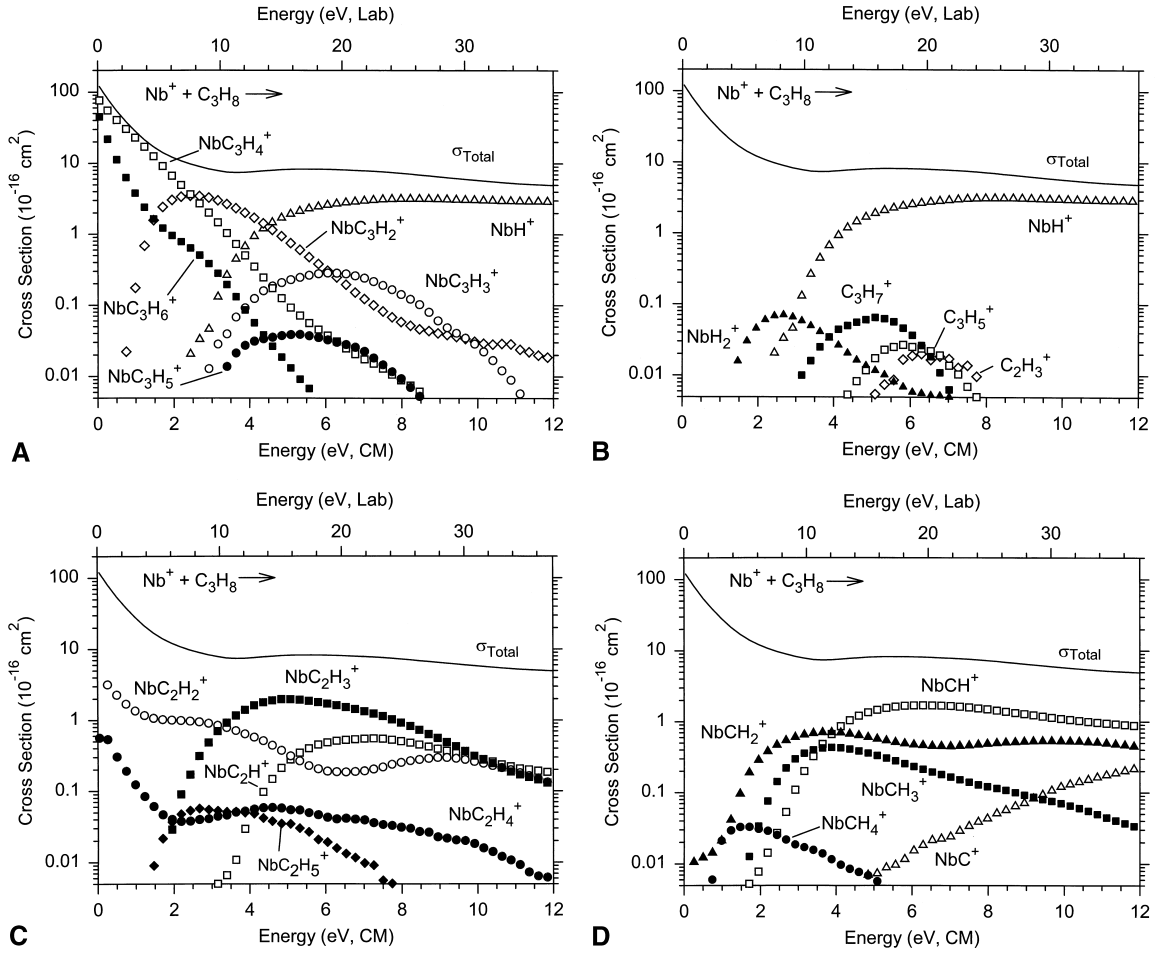

Fig. 3. Cross sections for reactions of Nb^+ with C_3H_8 as a function of kinetic energy in the center-of-mass frame (lower axis) and laboratory frame (upper axis). (a) Results for C–H bond cleavage reactions leading to $NbC_3H_x^+$ and NbH^+ products; (b) for C–H bond cleavage reactions leading to NbH_2^+, NbH^+, and hydrocarbon cation products; (c) for C–C bond cleavage reactions leading to $NbC_2H_x^+$ products; and (d) for C–C bond cleavage reactions leading to $NbCH_x^+$ products. The full lines in (a)–(d) show the total reaction cross section for all parts.

species accounts for 31% of the products at thermal energies (0.04 eV), but then falls off rapidly as $E^{-2.0\pm0.1}$ above 0.2 eV. The magnitude of this product is limited by the efficiency of double dehydrogenation to form $NbC_3H_4^+$ in reaction (31), a process that is also exothermic. This is indicated because both cross sections decline with increasing energy, consistent with exothermic processes having no barriers in excess of the energy of the reactants. Double dehydrogenation accounts for 66% of all products at thermal energies (0.04 eV). As the energy is increased above 0.6 eV, the $NbC_3H_4^+$ cross section drops more rapidly ($\sim E^{-1.5}$) as the $NbC_3H_2^+$ product is formed. This indicates that the slightly endothermic triple dehydrogenation, reaction (29), depletes the $NbC_3H_4^+$ product. Above about 3 eV, the $NbC_3H_6^+$, $NbC_3H_4^+$, and $NbC_3H_2^+$ product cross sections all begin to decline more rapidly. This is apparently caused by competition with the formation of NbH^+ in reaction (17) as no other product has a cross section with sufficient intensity to account for the declines. The sum of the $NbC_3H_6^+$, $NbC_3H_4^+$, $NbC_3H_2^+$, and NbH^+ cross sections decreases smoothly, thereby indicating that the latter reaction channel probably

depletes a common intermediate, as discussed below.

At higher energies, $NbC_3H_3^+$ and $NbC_3H_5^+$ are formed in reactions (30) and (32). These species must come from H atom loss from the $NbC_3H_4^+$ and $NbC_3H_6^+$ products. An alternate pathway is sequential dehydrogenation of a transiently formed $NbC_3H_7^+$ species, however the energy dependence observed is obviously not sequential in nature, i.e. $NbC_3H_3^+$ has a lower apparent threshold than $NbC_3H_5^+$. Evidence for the former pathway is the observation that the relative sizes of these cross sections are consistent with being limited by the size of $NbC_3H_4^+$ and $NbC_3H_6^+$ precursors. We cannot conclude this definitively, however, because at low energies, these cross sections are obscured by mass overlap with the other $NbC_3H_x^+$ products that are orders of magnitude more intense.

One reaction channel in direct competition with the major dehydrogenation processes is formation of NbH_2^+, reaction (18). As shown in Fig. 3(b), formation of this product is clearly endothermic. This cross section reaches a maximum very close to the threshold observed for NbH^+ formation, however, this cannot be because this species decomposes to NbH^+. This would be equivalent to the overall formation of $NbH^+ + H + C_3H_6$, which cannot occur until 3.41 ± 0.07 eV. Therefore, as in the ethane system, the NbH_2^+ cross section must decline at this energy because the NbH^+ channel depletes a common intermediate.

C–H bond cleavage can also form the neutral NbH molecule accompanied by the $C_3H_7^+$ product. The alkyl fragment $C_3H_7^+$ rises from an apparent threshold near 3 eV. The decline in the $C_3H_7^+$ cross section can be attributed to H_2 and CH_4 loss to form $C_3H_5^+$ and $C_2H_3^+$, respectively. The precipitous declines in these cross sections at higher energies is almost certainly the result of incomplete product ion collection. This indicates that these products have little forward velocity in the laboratory frame, consistent with simple abstraction of a hydride from propane by Nb^+.

The products formed by the cleavage of the C–C bond in the reaction of Nb^+ with propane are shown in Fig. 3(c) and (d). Of the various $NbC_2H_x^+$ products, two are formed in exothermic processes with no barriers in excess of the energy of the reactant. The less abundant of these is a primary product, $NbC_2H_4^+$, formed in reaction (27). This species accounts for only 0.4% of the products at thermal energies (0.04 eV). The cross section for this species rises again near 2 eV, which must correspond to the formation of $CH_3 + H$ instead of CH_4. The major C–C bond cleavage product at low energies is $NbC_2H_2^+$, formed in reaction (25), and hence a secondary product. This product accounts for 3% of the reactivity at thermal energies (0.04 eV). This species could be formed either by dehydrogenation of the $NbC_2H_4^+$ or demethanation of the $NbC_3H_6^+$ primary products. This cross section rises again near 6 eV, and this must correspond to $CH_3 + H + H_2$ or $CH_4 + 2$ H products.

The cross sections for $NbC_2H_3^+$ and $NbC_2H_5^+$ begin to rise near 1.5 eV. The $NbC_2H_5^+$ cross section reaches a maximum about 1 eV higher in energy because dehydrogenation of this product ion to form $NbC_2H_3^+$ is energetically allowed with little excess energy. A secondary decomposition channel is H atom loss, which yields the higher energy feature in the $NbC_2H_4^+$ cross section. The $NbC_2H_3^+$ cross section rises until near 5 eV and then declines primarily because of dehydrogenation to NbC_2H^+. A minor decomposition channel is probably H loss to form $NbC_2H_2^+$, resulting in the second feature in that cross section beginning near 6 eV. The NbC_2H^+ rises from an apparent threshold near 3.5 eV and continues rising until near 7 eV at which point it starts to decline because of further dissociation. The $NbC_2H_x^+$ (x = 5, 3, 1) products can all decline starting at $D_0(CH_3–C_2H_5) = 3.77$ eV, because the $NbC_2H_5^+$ species can decompose to $Nb^+ + C_2H_5$ starting at this energy. This probably accounts for the gradual decline in the sum of these cross sections above ~4 eV.

Fig. 3(d) shows ionic products containing Nb and a single carbon atom. Of these, the ones formed at the lowest energies are $NbCH_2^+$ and $NbCH_4^+$. The latter product competes directly with the exothermic formation of $NbC_2H_4^+$. The $NbCH_4^+$ product cross section rises from an apparent threshold below 1 eV and reaches a maximum at slightly higher energies, near the onset of the $NbCH_3^+$ channel. Analogous to the case of the NbH_2^+ product, this species cannot be decomposing to $NbCH_3^+ + H$ or $NbH^+ + CH_3$ at

Table 2
Optimized parameters of Eq. (1) for $Nb^+ + CH_4$ system

Reactants	Products	σ_0	n	E_0 (eV)
$Nb^+ + CH_4$	$NbH^+ + CH_3$	1.87 (0.16)	1.0 (0.2)	2.57 (0.09)
	$NbC^+ + 2H_2$	0.17 (0.07)	1.1 (0.5)	2.69 (0.22)
	$NbCH^+ + H_2 + H$	0.50 (0.22)	1.7 (0.4)	2.99 (0.22)
	$NbCH_2^+ + H_2$	2.15 (0.30)	0.8 (0.1)	0.21 (0.04)
	$NbCH_3^+ + H$	0.021 (0.006)	1.0 (0.4)	2.46 (0.25)
$Nb^+ + CD_4$	$NbD^+ + CD_3$	1.33 (0.28)	1.3 (0.2)	2.61 (0.12)
	$NbC^+ + 2D_2$	0.20 (0.11)	1.3 (0.3)	2.72 (0.14)
	$NbCD^+ + D_2 + D$	0.52 (0.25)	2.0 (0.5)	3.16 (0.24)
	$NbCD_2^+ + D_2$	1.42 (0.04)	0.8 (0.1)	0.31 (0.04)
	$NbCD_3^+ + D$	0.072 (0.014)	1.1 (0.3)	2.62 (0.14)

this energy. Rather the decline must be because a new channel is depleting the population of a common intermediate. The $NbCH_2^+$ cross section is finite at thermal energies, indicating the presence of an inefficient exothermic or thermoneutral channel. At about 1 eV, the cross section rises sharply and continues rising until near 4 eV where it reaches a maximum due to competition with other channels and dissociation. Dehydrogenation to NbC^+ can also occur but this pathway is inefficient. A second feature in the $NbCH_2^+$ cross section is also observed and can be attributed to neutral products of 2 CH_3 or $C_2H_5 + H$. $NbCH_3^+$ rises from an apparent threshold below 2 eV and falls off near 4 eV largely because of dehydrogenation to form $NbCH^+$. This secondary product rises from an apparent threshold near 2 eV and plateaus at higher energies.

In previous work on this system at thermal energies, Buckner et al. [14] observed the double and triple dehydrogenation processes, reactions (31) and (29), with a branching ratio of 85:15. No reaction efficiency was reported nor was the $NbC_3H_6^+$ product mentioned. Such a branching ratio is observed in our work [Fig. 3(a)] at a kinetic energy of almost 1.5 eV, where the other low energy products, $Nb(C_3H_6)^+$ and $Nb(C_2H_2)^+$, are less abundant than the two products observed in the ICR study.

4. Thermochemical results

The energy dependencies of the various cross sections are interpreted using Eq. (1). The optimum values of the parameters of Eq. (1) are listed for the methane, ethane, and propane systems in Tables 2–4. The threshold can then be related to thermodynamic information assuming that this represents the energy of the product asymptote, an assumption that is usually correct for ion–molecule reactions because of the long-range attractive forces. Thus, Eq. (37) is used to derive the BDEs provided below where RL is the reactant hydrocarbon.

$$D_0(Nb^+ - L) = D_0(R - L) - E_0 \quad (37)$$

Because our bond energy determination carefully includes all sources of reactant energy, the thermochemistry obtained is for 0 K. In previous work [32], we characterized the effective electronic temperature of Nb^+ ions formed in the flow tube source as <900 K (avg $E_{el} = 0.062$ eV) and likely to be 300 ± 100 K (avg $E_{el} = 0.024 \pm 0.008$ eV). The BDEs derived below are interpreted assuming the populations of the spin–orbit levels have a Maxwell-Boltzmann distribution at 300 K. It is possible that they could be up to 0.04 eV lower, well within the uncertainties listed, if 900 K better characterizes the ion temperature.

4.1. NbH^+

This product is formed in all three systems. A reliable value for $D_0(Nb^+–H)$, Table 1, has previously been determined from the reactions of Nb^+ with H_2 and D_2 [32]. This value is in good agreement with high level theoretical calculations [37–40], in particular those from Petersson et al. [38] and Das and

Table 3
Optimized parameters of Eq. (1) for $Nb^+ + C_2H_6$ system

Reactants	Products	σ_0	n	E_0 (eV)
$Nb^+ + C_2H_6$	$NbH^+ + C_2H_5$	1.62 (0.65)	1.8 (0.4)	2.36 (0.19)
	$NbH_2^+ + C_2H_4$	0.04 (0.01)	1.2 (0.3)	1.04 (0.19)
	$NbC^+ + CH_2 + 2H_2$	0.35 (0.17)	1.6 (0.3)	6.96 (0.30)
	$NbCH^+ + CH_3 + H_2$	4.58 (1.15)	1.6 (0.3)	2.63 (0.13)
	$NbCH_3^+ + CH_3$	1.67 (0.23)	1.7 (0.2)	1.77 (0.07)
	$NbC_2H^+ + 2H_2 + H$	0.64 (0.11)	1.3 (0.2)	4.41 (0.11)
	$NbC_2H_2^+ + 2H_2$	6.92 (0.90)	1.4 (0.3)	0.18 (0.06)
	$NbC_2H_3^+ + H_2 + H$	0.31 (0.14)	1.6 (0.4)	2.81 (0.24)

Balasubramanian [39]. Using this BDE, the predicted thresholds for the NbH^+ products are 2.20 ± 0.08, 2.03 ± 0.07, and 1.93 ± 0.07 eV for the CH_4, C_2H_6, and C_3H_8 systems, respectively, and given that $D_0(Nb^+–D) = 2.31 \pm 0.07$ eV [32], the predicted threshold for NbD^+ formation in the CD_4 system is 2.27 ± 0.07 eV. The thresholds measured for these processes, Tables 2–4, are all consistently higher than these predictions. This is apparently because of competition with more favorable dehydrogenation processes for each reaction system.

4.2. NbC^+

The thresholds obtained from the NbC^+ cross sections result in $D_0(Nb^+–C)$ of 5.37 ± 0.22 and 5.31 ± 0.14 eV for the CH_4 and CD_4 systems, respectively. These values agree within experimental error with the value of 5.16 ± 0.15 eV obtained by measuring the endothermicity of the $Nb^+ + CO \rightarrow NbC^+ + O$ reaction [33]. The average of these three values is 5.28 ± 0.15 eV and is our best experimental value at present. Hettich and Freiser [34] have observed photodissociation of $NbCH_2^+$ to NbC^+ at wavelengths out to at least 590 nm, such that $D_0(NbC^+–H_2) < 2.1$ eV (although data are shown only below 450 nm = 2.76 eV). Combined with our value for $D_0(Nb^+–CH_2)$ obtained below, the photodissociation result corresponds to $D_0(Nb^+–C) > 5.7$ eV (or more conservatively, >5.0 eV). As only the latter value agrees with the present results, we presume that the small photodissociation signals at long wavelengths are attributable to hot ions.

Table 4
Optimized parameters of Eq. (1) for $Nb^+ + C_3H_8$ system

Reactants	Products	σ_0	n	E_0 (eV)
$Nb^+ + C_3H_8$	$NbH^+ + C_3H_7$	2.03 (0.62)	1.9 (0.3)	2.81 (0.14)
	$NbH_2^+ + C_3H_6$	0.09 (0.04)	1.7 (0.3)	1.05 (0.06)
	$NbC^+ + C_2H_4 + 2H_2$	0.010 (0.006)	2.3 (0.4)	3.3 (0.4)
	$NbCH^+ + C_2H_5 + H_2$	1.50 (0.71)	1.9 (0.4)	2.60 (0.20)
	$NbCH_2^+ + C_2H_4 + H_2$	0.81 (0.10)	1.5 (0.2)	1.05 (0.07)
	$NbCH_3^+ + C_2H_5$	0.63 (0.30)	2.1 (0.8)	1.55 (0.24)
	$NbCH_4^+ + C_2H_4$	0.052 (0.011)	1.2 (0.3)	0.52 (0.11)
	$NbC_2H^+ + CH_3 + 2H_2$	1.08 (0.34)	1.4 (0.4)	3.91 (0.19)
	$NbC_2H_3^+ + CH_3 + H_2$	1.90 (0.85)	2.0 (0.4)	1.99 (0.18)
	$NbC_2H_4^+ + CH_3 + H$	0.13 (0.03)	0.8 (0.1)	2.5 (0.3)
	$NbC_2H_5^+ + CH_3$	0.11 (0.01)	1.3 (0.2)	1.32 (0.12)
	$NbC_3H_2^+ + 3H_2$	10.79 (0.82)	1.3 (0.3)	1.21 (0.08)
	$NbC_3H_3^+ + 2H_2 + H$	0.28 (0.07)	1.7 (0.2)	2.89 (0.12)
	$NbC_3H_5^+ + H_2 + H$	0.18 (0.03)	0.5 (0.2)	3.59 (0.08)
	$C_2H_3^+ + NbH + CH_4$	0.075 (0.011)	1.1 (0.2)	4.95 (0.09)
	$C_3H_5^+ + NbH + H_2$	0.097 (0.023)	1.1 (0.4)	4.24 (0.19)
	$C_3H_7^+ + NbH$	0.10 (0.04)	1.6 (0.5)	2.8 (0.2)

In the ethane and propane systems, there are mass overlap problems with the more intense $NbCH^+$ product channel making the detailed shape of the NbC^+ cross sections unreliable in the threshold region. In addition, there is some ambiguity about which neutral products correspond to the thresholds for NbC^+ reported in Tables 3 and 4. In the ethane system, the products most consistent with the threshold observed (Table 3) are $CH_2 + 2\ H_2$, which is predicted to have a threshold of 6.82 ± 0.15 eV. In the propane system, the products most consistent with the observed threshold are $C_2H_4 + 2H_2$, which should have a threshold of 3.58 ± 0.15 eV.

4.3. $NbCH^+$

As noted above, the mechanism for formation of $NbCH^+$ is dehydrogenation of the primary $NbCH_3^+$ product. The thresholds obtained from the $NbCH^+$ cross sections result in $D_0(Nb^+–CH)$ of 6.08 ± 0.22, 5.77 ± 0.13, and 5.77 ± 0.20 eV for the CH_4, C_2H_6, and C_3H_8 systems, respectively, and 5.91 ± 0.24 eV for $D_0(Nb^+–CD)$ in the CD_4 system. It seems possible that the thresholds for the ethane and propane systems are shifted slightly to higher energy because the neutral product formed in conjunction with $NbCH_3^+$ (methyl and ethyl radicals, respectively) carries away more energy than the H or D atom in the methane systems. For this reason, we average the two values obtained from methane systems (ignoring the small zero point energy differences) to obtain 6.02 ± 0.20 eV as our best value for $D_0(Nb^+–CH)$. Some confirmation of the accuracy of this value comes from agreement within experimental error with the 6.29 ± 0.34 eV value calculated from photodissociation results [34] (Table 1). More specifically, the photodissociation results directly obtain $D_0(NbCH^+–H)$ = 2.76 ± 0.22 eV. Combined with our value for $D_0(Nb^+–CH_2)$ obtained in Sec. 4.4, the photodissociation result corresponds to $D_0(Nb^+–CH)$ = 6.05 ± 0.24 eV, in excellent agreement with the value obtained here.

4.4. $NbCH_2^+$

The dominant reaction in the methane systems is dehydrogenation, reaction (5). This is clearly an endothermic process in both the CH_4 and CD_4 systems. Freiser and co-workers have demonstrated that the reverse reaction occurs readily at thermal energies, which shows that there is no barrier to this reaction in excess of the $NbCH_2^+ + H_2$ asymptote. Our measurements of the thresholds for reaction (5) result in $D_0(Nb^+–CH_2)$ = 4.52 ± 0.04 eV and for its deuterated analogue we obtain $D_0(Nb^+–CD_2)$ = 4.34 ± 0.04 eV. In the ethane and propane systems, the formation of $NbCH_2^+$ occurs inefficiently at thermal energies. These reactions correspond to formation of neutral products CH_4 and C_2H_6, respectively, and indicate that $D_0(Nb^+–CH_2) > 4.04$ and >4.17 eV. In the propane system, $NbCH_2^+$ is formed more efficiently at slightly higher energies and the analysis of this cross section feature is included in Table 4. The neutral products in this case must correspond to $C_2H_4 + H_2$, such that the measured threshold corresponds to $D_0(Nb^+–CH_2)$ = 4.46 ± 0.07 eV. These values are all quite consistent and we adopt the average of the three values for the methane and propane systems, 4.44 ± 0.09 eV for this product ion (ignoring the small zero point energy differences associated with the $NbCD_2^+$ value). This value agrees within experimental error with 4.60 ± 0.30 eV obtained by Hettich and Freiser [34] from the photodissociation threshold for $NbCH_2^+ \rightarrow Nb^+ + CH_2$. These authors revised their final estimate of this BDE to 4.73 ± 0.30 eV on the basis of observing reaction (5), even though they correctly concluded that this process is endothermic.

The experimental values greatly exceed the theoretical values calculated by Bauschlicher et al. [45], 3.86 ± 0.13 eV, and Siegbahn et al. [40], 4.12 eV. This is odd as agreement between our measured values and those calculated by Bauschlicher for other transition metal methylidene cations has generally been good [9,26–30]. Nevertheless, the data in the methane systems leaves no doubt that the $Nb^+–CH_2$ BDE cannot be this low. There are no barriers to these reactions in excess of the endothermicity (which

would raise the BDE anyway), as demonstrated by the efficiency of the reverse process [14,34]. The good agreement with the value obtained in the propane system where formation of $NbCH_2^+$ occurs by a different mechanism indicates that there are no obvious systematic effects in the determination of this BDE. The only possible means of lowering the experimentally determined BDE is if there are unaccounted sources of reactant energy, such as higher energy spin–orbit states that are much more reactive than lower energy spin-orbit states (which could lower the BDE by 0.13 eV at the very most). The presence of an excited state (e.g. $a\ ^5F$ at 0.42 eV) that is much more reactive with methane and propane than H_2 and D_2 could also be postulated, but there is no evidence for such an excited state in other reaction channels.

4.5. $NbCH_3^+$ and $NbC_2H_5^+$

The thresholds obtained for the $NbCH_3^+$ cross sections in the CH_4, C_2H_6, and C_3H_8 systems result in $D_0(Nb^+–CH_3)$ of 2.02 ± 0.25, 2.04 ± 0.07, and 2.22 ± 0.24 eV, respectively, and 1.96 ± 0.14 eV for $D_0(Nb^+–CD_3)$ in the CD_4 system. The average of these four values is 2.06 ± 0.11 eV, which compares very well with the theoretical value of 2.15 eV given by Bauschlicher et al. [43]. This identifies this species as the niobium methyl cation.

In the propane system, cleavage of the C–C bond yields $NbC_2H_5^+$ in competition with $NbCH_3^+$. Inspection of the data indicates that the threshold for process (28) is slightly below that for reaction (22), Fig. 3(c) and (d). Analysis of the $NbC_2H_5^+$ cross section is complicated because this product dehydrogenates at slightly higher energies to form $NbC_2H_3^+$. Nevertheless, similar thresholds are obtained whether we analyze the $NbC_2H_5^+$ cross section independently or the sum of the $NbC_2H_5^+$ and $NbC_2H_3^+$ cross sections. The results in Table 4 lead to $D_0(Nb^+–C_2H_5) = 2.45 \pm 0.12$ eV, 0.38 eV greater than $D_0(Nb^+–CH_3)$. This is comparable to results for the first-row congener of niobium, where $D_0(V^+–C_2H_5) = D_0(V^+–CH_3) + 0.33$ eV [9]. It is possible that the ground state geometry of $NbC_2H_5^+$ is not the niobium ethyl cation but rather $HNb(C_2H_4)^+$, a hydrido–ethene complex, but the thermochemistry cannot distinguish between these possibilities.

4.6. Bond-energy bond-order correlation for $Nb^+–CH_x$ bonds

One interesting way of investigating the bond order of simple metal ligand species is to compare with organic analogues, i.e. $D_0(Nb^+–L)$ versus $D_0(L–L)$ [73]. Such a plot is shown in Fig. 4, and differs somewhat from a previous version [34]. It can be seen that the correlation is remarkably good which indicates that $Nb^+–H$, $Nb^+–CH_3$, and $Nb^+–C_2H_5$ are all single bonds, $Nb^+{=}CH_2$ is a double bond, and $Nb^+{\equiv}CH$ is a triple bond. The bonding character of $Nb^+–O$ is discussed in detail elsewhere [33], but is predicted to have a bond order of three, and hence correlates with $D_0(C{\equiv}O)$. The point that lies furthest from the line is for $Nb^+–C$, correlated with the BDE of C_2. In this case, the NbC^+ BDE lies above the line because the covalent double bond in this molecule can be augmented by back donation of an occupied $4d\pi$ orbital on Nb^+ into the empty $2p\pi$ orbital on C, something that C_2 cannot do.

4.7. Products of dehydrogenation: $Nb(C_2H_x)^+$, $x = 2$ and 4, and $Nb(C_3H_x)^+$, $x = 2$, 4, and 6

Dehydrogenation of ethane and propane by Nb^+ is exothermic, indicating that $D_0(Nb^+–C_2H_4) > 1.34$ eV and that $D_0(Nb^+–C_3H_6) > 1.22$ eV. Loss of methane in the reaction with propane is also exothermic, which means that $D_0(Nb^+–C_2H_4) > 0.80$ eV. Somewhat more speculatively, we can model the exothermic part of the $NbC_2H_4^+$ cross section with a power law, subtract it from the experimental cross section and analyze the endothermic feature, Table 4. This yields $D_0(Nb^+–C_2H_4) = 2.8 \pm 0.3$ eV, in agreement with the lower limits and with the BDE to ethyne determined next.

Subsequent dehydrogenation of the $NbC_2H_4^+$ product formed in the propane system is also exothermic, giving $D_0(Nb^+–C_2H_2) > 2.54$ eV. Double dehydrogenation of ethane to form $NbC_2H_2^+$ is slightly endo-

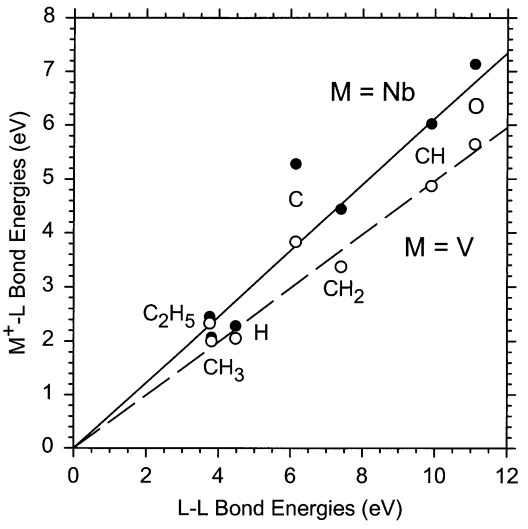

Fig. 4. Correlation of Nb^+–L and V^+–L bond energies with those for the organic analogues, L–L, except in the case of O where the bond energy of CO is used as the reference. Nb^+–L values are from Table 1, and V^+–L values are from [9]. Lines are linear regression fits to the data, excluding MC^+, constrained to pass through the origin.

thermic, with a measured threshold of 0.18 ± 0.06 eV. As noted above, collision-induced dissociation experiments on this product by Buckner et al. are consistent with the niobium–ethyne cation structure. The measured threshold (Table 3) can be converted to $D_0(Nb^+–C_2H_2) = 2.90 \pm 0.06$ eV, consistent with the lower limit obtained in the propane system. This BDE is somewhat greater than that measured by photodissociation [34] or calculated [47], Table 1. We note that the former value is inconsistent with the observation of exothermic formation of this product in the propane system. Further, the cross section for the endothermic double dehydrogenation of ethane cannot be accurately reproduced with a threshold as high as 0.6 eV (as predicted by a BDE of 2.47 eV) or 0.5 eV (as predicted by the theoretical BDE of 2.56 eV).

Double dehydrogenation of propane is exothermic, indicating that $D_0(Nb^+–C_3H_4) > 2.84$ eV, presuming that C_3H_4 has a propyne structure. This seems likely given that double dehydrogenation of ethane (also a relatively efficient process) occurs and gives the ethyne ligand. This BDE provides further experimental evidence that the Nb^+–ethyne bond is 2.90 eV. Triple dehydrogenation to form $NbC_3H_2^+$ is also observed as an endothermic process. Here, the difficulty is assigning a likely structure to this species although a reasonable possibility is the C=C=CH_2 biradical. Assuming this dissociation asymptote, the thermochemistry measured here provides a Nb^+=C_3H_2 BDE of 5.25 ± 0.19 eV. This is plausible as the Nb–C double bond can be augmented by delocalization of the C–C π electrons into an empty $d\pi$ orbital on niobium.

4.8. NbH_2^+ and $NbCH_4^+$

Two of the more interesting minor products observed in these systems are NbH_2^+ and $NbCH_4^+$, products that are not observed in the reactions of first-row transition metal cations with these alkanes. The NbH_2^+ product is formed in both C_2H_6 and C_3H_8 systems along with the appropriate alkene, ethene and propene, respectively. The thresholds obtained from the NbH_2^+ cross sections result in $D_0(Nb^+–H_2)$ of 0.30 ± 0.19 and 0.16 ± 0.06 eV, respectively. Because the cross section for this product is considerably larger in the propane system, it is much more reliably interpreted, as reflected in the smaller uncertainty. Therefore, we take this value as our best determination of this BDE. In the case of $NbCH_4^+$, formed in the C_3H_8 system [Fig. 3(d)], analysis of this cross section yields a threshold (Table 4) leading to $D_0(Nb^+–CH_4) = 0.30 \pm 0.11$ eV.

The key issue for these species is their structure, which can either be the inserted $Nb(H)_2^+$ and $Nb(H)(CH_3)^+$ species or the electrostatically bound molecular complexes, $Nb(H_2)^+$ and $Nb(CH_4)^+$. Bowers have measured the binding of H_2 to Nb^+ and determined a bond energy of 0.67 ± 0.04 eV [36]. Hence, the thermochemistry determined here for the NbH_2^+ product is inconsistent with this structure, although this presumes that there is no barrier to the formation of the NbH_2^+ species. This presumption must be correct, however, as there is no barrier observed to formation of Nb(alkene)$^+$, which would be formed by decomposition of the same (H_2)Nb(alkene)$^+$ intermediate leading to $Nb(H_2)^+$. Das and Balasubramanian [44] calculate that the

ground state of $Nb(H)_2^+$ is $^3B_2$ with a H–Nb–H bond angle of 105°; however, they calculate that this species lies 0.65 eV below the $Nb^+(a\ ^3F) + H_2$ excited state asymptote, which places it 0.34 eV *above* the $Nb^+(a\ ^5D) + H_2$ ground state asymptote. As the calculations failed to consider states evolving from the ground state asymptote, it is difficult to evaluate the accuracy of their conclusions.

Blomberg et al. [23] calculate that $Nb(H)(CH_3)^+$ has a $^3A''$ ground state with a H–Nb–C bond angle of 107.5°. They find that it also lies above $Nb^+(a\ ^5D) + CH_4$ (by 0.11 eV), but they carefully consider zero point energies and the limitations in their calculations and correct their binding energy to estimate that $Nb(H)(CH_3)^+$ is bound by 0.58 eV. Considering the estimates involved, this is in reasonable agreement with our experimental value of 0.30 ± 0.11 eV. They also calculate the BDE for the $Nb(CH_4)^+$ complex and obtain 0.77 eV (0.51 eV before correction), inconsistent with our thermochemistry. In contrast, Rosi et al. [46] calculate that the $Nb(CH_3)_2^+$ geometry is more stable than $Nb(C_2H_6)^+$. The dimethyl species has a $^3A_2$ ground state with a C–Nb–C bond angle of 97°. They calculate that $Nb(CH_3)_2^+$ lies 0.66 eV below the $Nb^+(a\ ^5D) + C_2H_6$ asymptote, while $Nb(C_2H_6)^+$ is estimated to be bound by 0.43 ± 0.22 eV. The extra stability of the dimethyl versus the dihydride and hydrido–methyl species is partly a function of the weaker C–C bond of ethane (3.8 eV) compared to the H_2 and H–CH_3 BDEs (4.5 eV).

Overall, the comparison with theory shows that the NbH_2^+ and $NbCH_4^+$ products can be plausibly assigned to either the covalently bound dihydride, $Nb(H)_2^+$, and hydrido–methyl, $Nb(H)(CH_3)^+$, complexes or electrostatically bound dihydrogen, $Nb(H_2)^+$, and methane, $Nb(CH_4)^+$, complexes. However, the comparisons are most consistent with the former structures. Experimentally, the simple fact that these species are observed provides further evidence for this assignment, a point that is discussed in the mechanisms section below.

Regardless of the structure of the NbH_2^+ and $NbCH_4^+$ species, the thermochemistry measured here can also be converted to $D_0(Nb^+–2H) = 4.64 \pm 0.06$ eV and $D_0[Nb^+–(H)(CH_3)] = 4.78 \pm 0.11$ eV. When these bond energy sums are combined with $D_0(Nb^+–H)$ and $D_0(Nb^+–CH_3)$, Table 1, one can also determine the second covalent bonds: $D_0(HNb^+–H) = 2.36 \pm 0.09$ eV, $D_0(HNb^+–CH_3) = 2.50 \pm 0.13$ eV and $D_0[(CH_3)Nb^+–H] = 2.71 \pm 0.20$ eV. In all cases, the second bond is stronger than the first, by only 0.08 for the dihydride and by 0.43 eV for the hydrido–methyl. This result agrees with the calculations of Rosi et al. [46] for $D_0(H_3CNb^+–CH_3)$ where the second methyl bond is 0.32 eV stronger than the first.

4.9. $NbC_2H_x^+$ ($x = 1$ and 3)

Various ionic products having the formula $NbC_2H_x^+$ are formed in the C_2H_6 and C_3H_8 systems. Those resulting from dehydrogenation ($x = 2$ and 4) or simple bond cleavage ($x = 5$) are discussed above. Subsequent dehydrogenation of the primary $NbC_2H_5^+$ product yields both $NbC_2H_3^+$ and NbC_2H^+. The thresholds obtained for the former species in the reactions with C_2H_6 and C_3H_8 give $D_0(Nb^+–C_2H_3)$ of 3.29 ± 0.24 and 3.57 ± 0.18 eV, respectively. We adopt the average value, 3.43 ± 0.21 eV, as our best value. Note that this BDE is greater than that for the single bond in $Nb^+–CH_3$, 2.06 ± 0.11 eV, but less than the double bond of $Nb^+–CH_2$, 4.44 ± 0.09 eV. As discussed elsewhere [9], transition metal ion bonds to vinyl can be strengthened by delocalization of the C–C π electrons to the metal center, i.e. a dative bond in addition to the covalent bond. For the early first-row transition metal cations (Ti^+, V^+, and Cr^+) where there is an empty orbital to accept these electrons, this bond to vinyl is 1.42 ± 0.35 eV stronger than the bond to methyl, very similar to the enhancement here of 1.37 ± 0.24 eV.

NbC_2H^+ is measured to have thresholds that yield $D_0(Nb^+–C_2H) = 4.36 \pm 0.11$ eV and 4.32 ± 0.19 eV in the ethane and propane systems, respectively. The very good agreement between the two values leads us to assign the mean value of 4.34 ± 0.19 eV to $D_0(Nb^+–C_2H)$. This bond energy is much stronger than $D_0(Nb^+–CH_3)$ and comparable to $D_0(Nb^+–CH_2)$, suggesting it has double bond character. Presuming that this species has a $Nb^+–C{\equiv}CH$ structure,

this can occur by delocalization of both pairs of C–C π electrons into the $d\pi$ orbitals on Nb^+, in essence forming two dative bonds in addition to the covalent Nb–C single bond.

4.10. $NbC_3H_x^+$, x = 3 and 5

Minor products observed in the propane system are $NbC_3H_x^+$ where $x = 3$ and 5, Fig. 3. At low energies, these cross sections are obscured by mass overlap with the other $NbC_3H_x^+$ products that are orders of magnitude more intense. In addition, competition with these other products could shift the thresholds for $NbC_3H_3^+$ and $NbC_3H_5^+$ to higher energies. Thus, the thresholds for these products should be considered as upper limits. Analysis of the cross sections after correction for mass overlap yields the results in Table 4. The threshold obtained for the $NbC_3H_5^+$ cross section in the C_3H_8 system yields a BDE of $D_0(Nb^+–C_3H_5) \geq 1.39 \pm 0.08$ eV, given that dissociation forms the allyl radical. This implies nothing about the structure of the complex, although an allyl ligand is certainly reasonable. This value seems quite low compared with BDEs for other radicals bound to Nb^+, which suggests that the thermodynamic threshold is not observed in this case. The $NbC_3H_3^+$ product is also observed in an endothermic reaction in this system. The threshold corresponds to $D_0(Nb^+–C_3H_3) \geq 3.76 \pm 0.23$ eV if dissociation yields a CH_2CCH structure, which also implies nothing about the structure of the complex. This value is comparable to the BDE for $NbC_2H_3^+$, which has a single covalent Nb–C bond augmented by π interactions.

4.11. NbH

In the propane system, the $C_2H_3^+$, $C_3H_5^+$, and $C_3H_7^+$ species are formed in reactions along with NbH. When combined with literature thermochemistry for the hydrocarbon ions and the ionization energy of niobium, IE(Nb) = 6.759 eV [74], the measured thresholds for these reactions result in $D_0(Nb–H) = 2.3 \pm 0.1$, 2.0 ± 0.2, and 2.0 ± 0.2 eV, respectively. As for the formation of the competitive $NbH^+ + C_3H_7$ channel, these values are lower limits because of the strong competition with the exothermic dehydrogenation processes. Hence, we conclude that $D_0(Nb–H) > 2.3 \pm 0.1$ eV, in agreement with the calculated values of 2.55 and 2.56 eV [41–43].

5. Discussion

5.1. Reaction mechanism

The activation of alkanes by transition metal cations is generally explained using an oxidative addition mechanism in which M^+ inserts into a C–H or C–C bond to form $R–M^+–H$ or $R'–M^+–CH_3$ intermediates [1,2,25]. Products can be formed by reductive elimination of small molecules such as H_2 and CH_4 at low energies, and by metal–hydrogen or metal–carbon bond cleavage at high energies. The elimination processes can occur either by multicenter transition states or by rearrangement of the intermediate through β-H or β-CH_3 transfers to form $(H)_2M^+(C_xH_{2x})$ or $(CH_3)(H)M^+(C_xH_{2x})$ species, which then reductively eliminate H_2 or CH_4, respectively. This general mechanism has also been invoked to interpret experimental observations for the reactions of the first-row transition metal congener, V^+, with alkanes [50,58–60]. Among the key issues in determining the detailed mechanism is the spin states of the reactant, intermediates, and products and the stabilities of two types of possible intermediates: (1) $R–Nb^+–H$ and $R'–Nb^+–CH_3$, and (2) $(H)_2Nb^+(C_xH_{2x})$ and $(CH_3)(H)Nb^+(C_xH_{2x})$.

The reactants have a quintet spin state, $Nb^+(^5D) + C_xH_{2x+2}$ (^1A). Calculations indicate that the ground state of NbH^+ is $^4\Delta$ [38,39], $NbCH_3^+$ is $^4A_2$ [43], $NbCH_2^+$ is $^3B_2$ [45], $Nb(H)_2^+$ is $^3B_2$ [44], and $Nb(H)(CH_3)^+$ is $^3A''$ [23]. All other primary products involve an alkene or alkyne bound to Nb^+. $Nb(C_2H_2)^+$ is calculated to have a $^3A_2$ ground state [47]. Calculations have not been performed for $Nb(C_2H_4)^+$, but comparison with results for analogous complexes of V [47,75] suggest that it also has a triplet ground state. Thus, formation of the $NbH^+ + C_xH_{2x+1}$ and $NbCH_3^+ + C_{x-1}H_{2x-1}$ products is spin allowed, whereas formation of all other primary products is spin forbidden. We can also determine that

the R–Nb^+–H and R′–Nb^+–CH_3 intermediates should have triplet spins, in direct analogy with $Nb(H)_2^+$ and $Nb(H)(CH_3)^+$. Likewise, the possible $(H)_2Nb^+(C_xH_{2x})$ and $(CH_3)(H)Nb^+(C_xH_{2x})$ intermediates should have triplet ground states. In all three alkane systems, this indicates that there is a change in spin from quintet to triplet as the reactants interact strongly with the alkane to form the R–Nb^+–H and R′–Nb^+–CH_3 intermediates. On the basis of the present results, it appears that this spin conversion is fairly efficient in the niobium systems. All subsequent rearrangements and the formation of all products can then evolve along triplet surfaces.

As discussed above in Sec. 4.1.8, our present experimental results coupled with theoretical calculations indicate that the H–Nb^+–CH_3 intermediate is stable compared to the $Nb^+ + CH_4$ reactants and $Nb^+(CH_3)_2$ is stable compared to $Nb^+ + C_2H_6$ reactants. Likewise we can conclude that all possible R–Nb^+–H and R′–Nb^+–CH_3 intermediates should also be stable compared to the reactants because the R–H and R′–CH_3 bonds are no stronger than H–CH_3 and the replacement of the methyl group by a larger alkyl should only stabilize the intermediate further.

Blomberg et al. also calculate the energy of the transition state connecting $Nb(CH_4)^+$ with H–Nb^+–CH_3 finding a value of 0.24 eV (0.93 eV before correction for zero point, basis set, and correlation effects) above the energy of the $Nb^+ + CH_4$ reactants [23]. This is comparable to the thresholds we observe for dehydrogenation of methane (Table 2), suggesting that this threshold might correspond to the energy of this oxidative addition transition state rather than to the $NbCH_2^+ + H_2$ product asymptote. However, this would mean that the Nb^+–CH_2 BDE is larger than the experimental value given in Table 1, making the disagreement with theoretical calculations even larger. Further, such a barrier is inconsistent with the observation of an efficient reverse reaction by Freiser and co-workers [14,34]. Hence we conclude that the energy of this transition state cannot lie higher than the $NbCH_2^+ + H_2$ products, which lie only slightly higher than the $Nb^+ + CH_4$ reactants. This conclusion also translates to the ethane and propane systems, again because of the variations in thermochemistry expected as the hydrocarbon gets larger, and because these systems exhibit processes at thermal energies that are efficient and barrierless.

As noted above, there is strong competition observed between the formation of the thermodynamically favored products, e.g. $NbCH_2^+ + H_2$, $NbC_2H_4^+ + H_2$, and $NbC_3H_6^+ + H_2$, and the $NbH^+ + R$ products. A key observation is that the decline in the cross sections of the former products is compensated by the increase in the NbH^+ cross section. Although contributions of direct abstraction processes to the formation of NbH^+ cannot be excluded, such a mechanism is unlikely to compete so efficiently with the dehydrogenation channels. However, if these processes share a common intermediate and $NbH^+ + R$ formation is kinetically favored, then this process will rapidly deplete the intermediate before the more complicated dehydrogenation reactions can occur. The H–Nb^+–R intermediate is an obvious choice as NbH^+ formation can occur by simple bond cleavage at elevated kinetic energies, whereas H_2 elimination must occur by a more restricted transition state. Thus, the existence of this intermediate is not in question for Nb^+ reacting with any alkane. Likewise, the existence of CH_3–Nb^+–R′ intermediates seems certain as these lead to the primary $NbCH_3^+$ and $NbC_2H_5^+$ products observed in the ethane and propane systems. The mechanisms responsible for the dehydrogenation and alkane elimination reactions observed at low energy are more difficult to determine and are discussed in the following sections.

5.2. Mechanism for reaction with methane

Blomberg et al. [23] calculate that the elimination of H_2 from H–Y^+–CH_3 occurs by passing over a four-center transition state, calculated to lie about 0.43 eV below the energy of the products. It seems reasonable that a similar mechanism is followed for niobium and that the relative energetics are not that different. Another way of understanding this step is to consider the reverse reaction, i.e. H_2 activation by $NbCH_2^+$. The following discussion is consistent with simple molecular orbital ideas developed for the

activation of H_2 and CH_4 by metal oxide ions [76]. As discussed in detail elsewhere [2,3], activation of covalent bonds at transition metal centers is most facile when the metal has an empty *s*-like valence orbital to accept the pair of electrons in the covalent bond, and when it has a pair of valence $d\pi$-like electrons to donate into the antibonding orbital of the bond to be broken. For the metal methylidenes, the valence molecular orbitals (MOs) are $1a_1$ and $1b_1$ M–C bonding; $1a_2$, $1b_2$, and $2a_1$ *d*-like nonbonding; a $3a_1$ *s*-like nonbonding; and $2b_1$ and $4a_1$ antibonding orbitals. For these species, the most likely acceptor orbital is the $3a_1$ MO and the π-donor orbital is one of the nonbonding MOs. The ground state of $NbCH_2^+$ is $^3B_2$ with a $(1a_1)^2(1b_1)^2(1a_2)^0(1b_2)^1(2a_1)^1(3a_1)^0$ electron configuration and there should be a low-lying $^3B_1$ state with a configuration of $(1a_1)^2(1b_1)^2(1a_2)^1(1b_2)^1(2a_1)^0(3a_1)^0$ [45]. Note that neither of these states occupy the $3a_1$ acceptor orbital. Thus, the interaction of ground state $NbCH_2^+$ with H_2 is attractive and allows facile activation of H_2 across the Nb–C bond to form $H–Nb^+–CH_3$.

At higher energies, the $H–Nb^+–CH_3$ intermediate decomposes by cleavage of the Nb–H and Nb–C bonds to form the primary $NbCH_3^+$ and NbH^+ products. Although these channels have similar energetics, the latter product is favored as it can conserve angular momentum more easily [59]. At higher energies, NbC^+ and $NbCH^+$ are formed by subsequent dehydrogenation and H atom loss processes from the primary $NbCH_2^+$ and $NbCH_3^+$ products. The thermochemistry determined above shows that dehydrogenation of these species requires 2.51 ± 0.17 and 0.64 ± 0.26 eV, respectively. The large difference is because the formal bond order changes little in going from $Nb^+{=}CH_2$ to $Nb^+{=}C$ but changes from 1 to 3 in the transition from $Nb^+–CH_3$ to $Nb^+{\equiv}CH$, Fig. 4. It is interesting to note that H atom loss from $NbCH_3^+$, which leads to the second features in the $NbCH_2^+$ cross sections, Figs. 1, 2(b), and 3(d), requires 2.34 ± 0.19 eV. This process is still observed even though dehydrogenation is a much lower energy channel. This indicates that H atom loss is kinetically more favorable than H_2 elimination, as expected.

5.3. Dehydrogenation of ethane and propane

Dehydrogenation of the larger alkanes can proceed by initial C–H bond activation to form $H–Nb^+–C_xH_{2x+1}$. This intermediate can then rearrange through a multicenter transition state in which a β-H interacts directly with the H on the metal to yield a $(H_2)Nb^+(C_xH_{2x})$ complex. Alternatively, the β-H first transfers to the metal to form $(H)_2Nb^+(C_xH_{2x})$ which then reductively eliminates H_2, again forming $(H_2)Nb^+(C_xH_{2x})$. This latter product generally loses the H_2 ligand, as it is bound much less strongly than the alkene (BDEs of 0.67 versus 2.8 eV, Table 1). Indeed, this large difference in binding energies makes it implausible (although not impossible) that a significant amount of $Nb(H_2)^+$ could be generated by competitive loss of the alkene. It seems more likely that the alkene could be lost from a $(H)_2Nb^+(C_xH_{2x})$ intermediate, as alkene loss (while still thermodynamically disfavored) is a simple bond cleavage reaction and hence kinetically more favorable than H_2 elimination, which requires reductive elimination involving a tight transition state. Thus, the observation of NbH_2^+ products in both the ethane and propane systems provides circumstantial evidence for the pathway involving the $(H)_2Nb^+(C_xH_{2x})$ intermediate.

5.4. Alkane elimination from ethane and propane

Two types of alkane elimination processes are observed for the larger alkanes studied here, formation of $NbCH_2^+ + C_{x-1}H_{2x}$ in the ethane and propane systems and of $Nb(C_2H_4)^+ + CH_4$ in the propane system. The former reaction is likely to follow the same type of mechanism as the formation of $NbCH_2^+$ in the methane system. Specifically, elimination of RH from a $H–Nb^+–CH_2–R$ intermediate or elimination of R′H from a $H_3C–Nb^+–R'$ intermediate, both passing through four-center transition states. These processes probably account for the exothermic formation of $NbCH_2^+$ at the lowest energies in both systems [Figs. 2(b) and 3(d)]. They are less efficient than the reaction in the methane system because there is no competition with other more favorable reactions in the latter system and the four-center transition state is

probably more restricted when an alkyl group rather than an H atom is involved.

The formation of $Nb(C_2H_4)^+ + CH_4$ in the propane system is interesting as this C–C bond activation process can be fairly efficient for many metal cations [2,3], in particular, the late first-row transition metal cations. In analogy with the dehydrogenation process, it seems likely that this reaction occurs by initial C–C bond activation to form $H_3C–Nb^+–C_2H_5$, followed by a β-H shift to yield the $(CH_3)(H)Nb^+(C_2H_4)$ intermediate, which then reductively eliminates methane. The observation of the $Nb(H)(CH_3)^+$ product [Fig. 3(d)] is taken as evidence for this latter intermediate, using parallel arguments to those for the analogous $(H)_2Nb^+(C_3H_6)$ intermediate. Alternatively, initial primary C–H bond activation to form $H–Nb^+–C_3H_7$ followed by a β-CH_3 shift yields the same $(CH_3)(H)Nb^+(C_2H_4)$ intermediate. These two pathways cannot be distinguished on the basis of the present experiments, although recent calculations suggest that β-alkyl migrations are higher energy pathways than β-H shifts [57]. If the former pathway is active, then the inefficiency of methane elimination (C–C bond cleavages account for only 3% of the total reactivity at thermal energies) can be explained by the relative amounts of initial C–H versus C–C bond activation. This is presumably controlled by the relative energies of the insertion transition state. If the latter pathway is active, then the relative efficiencies of the β-H versus β-CH_3 shifts is probably determining.

5.5. Reactivity differences between Nb^+ and V^+

The kinetic energy dependencies of the reactions of V^+ (the first-row transition metal congener of Nb^+) with CH_4, C_2H_6, and C_3H_8 have been studied previously [50,58–64]. The differences in the reactivity of V^+ and Nb^+ can be summarized fairly succinctly. First, the efficiency of the dehydrogenation processes differs dramatically between the two metals. Reactions (16) and (31) + (33) are exothermic and efficient, occurring on nearly every collision, while reaction (5) is endothermic, but still has an appreciable cross section. In contrast, the corresponding reactions in the V^+ systems are much less efficient, and observed at thermal energies only in the propane system. Here, the reaction is barrierless but occurs in only 1 of every 200 collisions [50,63]. Second, exothermic elimination of methane from propane, reaction (27), is inefficient for Nb^+ but occurs at thermal energies. For V^+, this exothermic process exhibits a barrier of 0.70 ± 0.06 eV [50]. Third, subsequent dehydrogenation of primary products (forming species such as NbC^+, $NbCH^+$, NbC_2H^+, $NbC_2H_2^+$, $NbC_2H_3^+$, $NbC_3H_2^+$, $NbC_3H_3^+$, $NbC_3H_4^+$, and $NbC_3H_5^+$) is pronounced in the niobium systems. Analogous processes are observed in the vanadium systems but are much less efficient.

Most of these differences in reactivity can be understood simply on the basis of differences in thermochemistry. The hydride and methyl BDEs of vanadium and niobium cations are similar; compare $D_0(V^+–H) = 2.05 \pm 0.06$ eV and $D_0(V^+–CH_3) = 2.00 \pm 0.07$ eV [9] with the values in Table 1. In contrast, the NbC^+, $NbCH^+$, $NbCH_2^+$ bonds are stronger than the vanadium analogues by 1.2 ± 0.2 eV [9]. These bond energies are also compared in Fig. 4. Likewise, the $Nb^+–C_2H_4$ BDE exceeds that for $V^+–C_2H_4$ [77] by 1.5 ± 0.3 eV, and Sodupe and Bauschlicher [47] have calculated that $D_0(Nb^+–C_2H_2)$ is greater than $D_0(V^+–C_2H_2)$ by 1.0 eV. Similar results should hold for all other alkene and alkyne complexes. Thus, formation of all products but MH^+ and $M(alkyl)^+$ are energetically more favorable in the niobium system by 1 eV or more. This clearly explains the third difference noted above, the relative efficiency of the subsequent dehydrogenation processes. To a large extent, these energy differences also explain the first point, the differences in the primary dehydrogenation channels. Dehydrogenation of all three alkanes by V^+ is energetically more costly than when induced by Nb^+, sufficiently so that $VC_2H_4^+$ formation is endothermic in the V^+ + ethane system. However, dehydrogenation of propane by both metal cations is exothermic and has no barriers in excess of the energy of the reactants, hence the two order of magnitude difference in efficiencies for this process requires additional considerations.

As discussed previously [50], the inefficiency of

the dehydrogenation of propane by V^+ has been attributed to intermediates that lie only slightly below the energy of the reactants and the need to couple from a quintet reactant surface to a triplet intermediate surface and back to a quintet product surface. [Unlike $Nb(C_3H_6)^+$, which has a triplet ground state, see discussion above, $V(C_3H_6)^+$ has a quintet ground state, necessitating two spin changes for this reaction: one in the entrance channel and one in the exit channel.] In the case of Nb^+, the intermediates should be more stable: $D_0[Nb^+–(H)(CH_3)] = 4.78 \pm 0.11$ eV versus $D_0[V^+–(H)(CH_3)] = 4.04 \pm 0.16$ eV [9,60]. Further, because the $M(C_3H_6)^+$ products have different spins for the two metals, there is no spin change in the exit channel for Nb, and the spin–orbit coupling necessary to mix the quintet and triplet surfaces in the entrance channel should be more effective for the heavier metal. Part of the reason for these differences is that the lowest-lying triplet state of the atomic ion is lower in energy for Nb^+. The excitation energy of the $^3P(4d^4)$ state of Nb^+ is 0.833 eV [78], compared to the $^3F(4s^13d^3)$ state of V^+, which lies 1.10 eV above the ground state [79].

Finally, the elimination of methane from propane to form $M(C_2H_4)^+$ exhibits a barrier of 0.70 ± 0.06 eV for M = V. Two explanations for this barrier were discussed [50]. First, the barrier could correspond to the energy where the quintet and triplet surfaces cross in the exit channel. This is no longer a problem for M = Nb, again because of the difference in the spin of the ground states of $V(C_2H_4)^+$ and $Nb(C_2H_4)^+$. Second, the barrier could correspond to the transition state for methane elimination on the triplet surface. The transition state in question converts the $H–M^+–C_3H_7$ intermediate to the $(H)(CH_3)M^+(C_2H_4)$ intermediate by β-CH_3 transfer. Relative to reactants, the $Nb(H)(CH_3)^+$ intermediate is more stable than $V(H)(CH_3)^+$ by 0.74 ± 0.20 eV. Thus, it is feasible that the comparable barrier for the niobium system lies slightly below the energy of the reactants. In such an event, even though there is no barrier above the energy of the reactants, a barrier just below could explain the inefficiency of this reaction in the Nb system.

6. Conclusion

Ground state Nb^+ ions are found to be very reactive with CH_4, C_2H_6, and C_3H_8 over a wide range of kinetic energies. Efficient dehydrogenation is observed at low energies in all three reaction systems, while alkane elimination is nearly absent in the latter two systems. At high energies, the dominant process in the methane, ethane, and propane systems is C–H bond cleavage to form $NbH^+ + R$, although there are also appreciable contributions from $NbCH_3^+$ and $NbC_2H_5^+$ and products that result from dehydrogenation of these primary products, $NbCH^+$ and $NbC_2H_3^+$. The endothermic reaction cross sections observed in all three systems are modeled to yield 0 K bond dissociation energies for several Nb–ligand cations, as summarized in Table 1. Reasonable agreement is found for these values compared with previous experimental and theoretical work, although theory is found to underestimate the $Nb^+–CH_2$ and $Nb^+–C_2H_2$ bond energies. Lower limits to Nb^+–alkene and Nb^+–alkyne BDEs are established by the observation of exothermic dehydrogenation reactions.

Possible mechanisms for the reactions of Nb^+ with these hydrocarbons are discussed in some detail. A key observation in the present system is the formation of NbH_2^+ and $NbCH_4^+$ species, proposed to be the covalently bound dihydride and hydrido–methyl complexes. These considerations suggest that the mechanisms of Nb^+ involve initial C–H or C–C bond activation followed by rearrangements to form $(H)(R)Nb^+$(alkene) intermediates. When compared to V^+, the first-row transition metal congener, Nb^+ is found to be much more reactive. This can be attributed to much stronger π bonds for the second-row metal ion and to more efficient coupling between surfaces of different spin.

Acknowledgement

This research is supported by the National Science Foundation, grant nos. CHE-9530412 and CHE-9877162.

References

[1] J. Allison, Prog. Inorg. Chem. 34 (1986) 627; R.R. Squires, Chem. Rev. 87 (1987) 623; Gas Phase Inorganic Chemistry, D.H. Russell (Ed.), Plenum, New York, 1989; K. Eller, H. Schwarz, Chem. Rev. 91 (1991) 1121.

[2] For reviews, see P.B. Armentrout, in Selective Hydrocarbon Activation: Principles and Progress, J.A. Davies, P.L. Watson, A. Greenberg, J.F. Liebman (Eds.), VCH, New York, 1990, p. 467; P.B. Armentrout, in Gas Phase Inorganic Chemistry, D.H. Russell (Ed.), Plenum, New York, 1989, p. 1; P.B. Armentrout, J.L. Beauchamp, Acc. Chem. Res. 22 (1989) 315.

[3] For reviews, see P.B. Armentrout, Science 251 (1991) 175; Annu. Rev. Phys. Chem. 41 (1990) 313.

[4] J.C. Weisshaar, Adv. Chem. Phys. 82 (1992) 213; Acc. Chem. Res. 26 (1993) 213.

[5] A.M. van Koppen, P.R. Kemper, M.T. Bowers, J. Am. Chem. Soc. 114 (1992) 1083, 10941; in Organometallic Ion Chemistry, B.S. Freiser (Ed.), Kluwer, Dordrecht, 1995, pp. 157–196.

[6] P.B. Armentrout, R. Georgiadis, Polyhedron 7 (1988) 1573.

[7] P.B. Armentrout, ACS Symp. Ser. 428 (1990) 18.

[8] P.B. Armentrout, D.E. Clemmer, in Energetics of Organometallic Species, J.A.M. Simoes, J.L. Beauchamp (Eds.), Kluwer, Dordrecht, 1992, p. 321.

[9] P.B. Armentrout, B.L. Kickel, in Organometallic Ion Chemistry, B.S. Freiser (Ed.), Kluwer, Dordrecht, 1995, pp. 1–45.

[10] Organometallic Ion Chemistry, B.S. Freiser (Ed.), Kluwer, Dordrecht, 1995.

[11] R.H. Crabtree, Chem. Rev. 85 (1985) 245.

[12] G.D. Byrd, B.S. Freiser, J. Am. Chem. Soc. 104 (1982) 5944.

[13] Y. Huang, M.B. Wise, D.B. Jacobson, B.S. Freiser, Organometallics 6 (1987) 346.

[14] S.W. Buckner, T.J. MacMahon, G.D. Byrd, B.S. Freiser, Inorg. Chem. 28 (1989) 3511.

[15] S.W. Buckner, B.S. Freiser, J. Am. Chem. Soc. 109 (1987) 1247.

[16] J.R. Gord, B.S. Freiser, S.W. Buckner, J. Chem. Phys. 91 (1989) 7530.

[17] Y.A. Ranasinghe, T.J. MacMahon, B.S. Freiser, J. Phys. Chem. 95 (1991) 7721.

[18] M.L. Mandich, L.F. Halle, J.L. Beauchamp, J. Am. Chem. Soc. 106 (1984) 4403.

[19] M.A. Tolbert, M.L. Mandich, L.F. Halle, J.L. Beauchamp, J. Am. Chem. Soc. 108 (1986) 5675.

[20] M.A. Tolbert, J.L. Beauchamp, J. Phys. Chem. 90 (1986) 5015.

[21] J.B. Schilling, J.L. Beauchamp, Organometallics 7 (1988) 194.

[22] B.L. Kickel, P.B. Armentrout, J. Am. Chem. Soc. 117 (1995) 4057.

[23] M.R.A. Blomberg, P.E.M. Siegbahn, M. Svensson, J. Phys. Chem. 98 (1994) 2062.

[24] M.R.A. Blomberg, P.E.M. Siegbahn, M. Svensson, J. Wennerberg, Journal of Energetics of Organometallic Species, J.A. Martinho Simoes (Ed.), Kluwer, Dordrecht, 1992, pp. 387–421.

[25] P.B. Armentrout, in Topics in Organometallic Chemistry, Vol. 4-I, J.M. Brown, P. Hofmann (Eds.), Springer-Verlag, Berlin, 1999, pp. 1–46.

[26] L.S. Sunderlin, P.B. Armentrout, J. Am. Chem. Soc. 111 (1989) 3845.

[27] P.B. Armentrout, Y.-M. Chen, J. Am. Soc. Mass Spectrom. 10 (1999) 821.

[28] Y.-M. Chen, P.B. Armentrout, J. Phys. Chem. 99 (1995) 10775.

[29] Y.-M. Chen, P.B. Armentrout, J. Am. Chem. Soc. 117 (1995) 9291.

[30] Y.-M. Chen, M.R. Sievers, P.B. Armentrout, Int. J. Mass Spectrom. Ion Processes 167/168 (1997) 195.

[31] Y.-M. Chen, P.B. Armentrout, J. Phys. Chem. 99 (1995) 11424.

[32] M.R. Sievers, Y.-M. Chen, J.L. Elkind, P.B. Armentrout, J. Phys. Chem. 100 (1996) 54.

[33] M.R. Sievers, Y.-M. Chen, P.B. Armentrout, J. Chem. Phys. 105 (1996) 6322.

[34] R.L. Hettich, B.S. Freiser, J. Am. Chem. Soc. 109 (1987) 3543.

[35] D.R.A. Ranatunga, B.S. Freiser, Chem. Phys. Lett. 233 (1995) 319.

[36] M.T. Bowers, unpublished work.

[37] J.B. Schilling, W.A. Goddard III, J.L. Beauchamp, J. Am. Chem. Soc. 109 (1987) 5565.

[38] L.G.M. Pettersson, C.W. Bauschlicher Jr., S.R. Langhoff, H. Partridge, J. Chem. Phys. 87 (1987) 481.

[39] K.K. Das, K. Balasubramanian, J. Mol. Spectrosc. 148 (1991) 250.

[40] P.E.M. Siegbahn, M.R.A. Blomberg, M. Svensson, Chem. Phys. Lett. 223 (1994) 35.

[41] S.R. Langhoff, L.G.M. Pettersson, C.W. Bauschlicher Jr., J. Chem. Phys. 86 (1987) 268.

[42] K.K. Das, K. Balasubramanian, J. Mol. Spectrosc. 144 (1990) 245.

[43] C.W. Bauschlicher Jr., S.R. Langhoff, H. Partridge, L.A. Barnes, J. Chem. Phys. 91 (1989) 2399.

[44] K.K. Das, K. Balasubramanian, J. Chem. Phys. 91 (1989) 6254.

[45] C.W. Bauschlicher Jr., H. Partridge, J.A. Sheehy, S.R. Langhoff, M. Rosi, J. Phys. Chem. 96 (1992) 6969.

[46] M. Rosi, C.W. Bauschlicher Jr., S.R. Langhoff, H. Partridge, J. Phys. Chem. 94 (1990) 8656. Adjusted value cited in [10].

[47] M. Sodupe, C.W. Bauschlicher Jr., J. Phys. Chem. 95 (1991) 8640.

[48] P.A.M. van Koppen, J. Brodbelt-Lustig, M.T. Bowers, D.V. Dearden, J.L. Beauchamp, E.R. Fisher, P.B. Armentrout, J. Am. Chem. Soc. 112 (1990) 5663; 113 (1991) 2359.

[49] P.A.M. van Koppen, M.T. Bowers, E.R. Fisher, P.B. Armentrout, J. Am. Chem. Soc. 116 (1994) 3780.

[50] P.A.M. van Koppen, M.T. Bowers, C.L. Haynes, P.B. Armentrout, J. Am. Chem. Soc. 120 (1998) 5704.

[51] C.L. Haynes, E.R. Fisher, P.B. Armentrout, J. Phys. Chem. 100 (1996) 18300.

[52] R.J. Noll, S.S. Yi, J.C. Weisshaar, J. Phys. Chem. 102 (1998) 386.

[53] J.K. Perry, Ph.D. Thesis, Caltech, 1994.

[54] M.C. Holthausen, A. Fiedler, H. Schwarz, W. Koch, J. Phys. Chem. 100 (1996) 6236.
[55] M.C. Holthausen, W. Koch, Helv. Chim. Acta 79 (1996) 1939.
[56] M.C. Holthausen, W. Koch, J. Am. Chem. Soc. 118 (1996) 9932.
[57] S.S. Yi, M.R.A. Blomberg, P.E.M. Siegbahn, J.C. Weisshaar, J. Phys. Chem. 102 (1998) 395.
[58] N. Aristov, P.B. Armentrout, J. Am. Chem. Soc. 108 (1986) 1806.
[59] N. Aristov, P.B. Armentrout, J. Phys. Chem. 91 (1987) 6178.
[60] N. Aristov, Ph.D. Thesis, University of California, Berkeley, 1986.
[61] L. Sanders, S. Hanton, J.C. Weisshaar, J. Phys. Chem. 91 (1987) 5145.
[62] S. Hanton, L. Sanders, J.C. Weisshaar, J. Phys. Chem. 93 (1989) 1963.
[63] L. Sanders, S. Hanton, J.C. Weisshaar, J. Chem. Phys. 92 (1990) 3498.
[64] M.R. Sievers, N. Aristov, P.B. Armentrout, unpublished work.
[65] K.M. Ervin, P.B. Armentrout, J. Chem. Phys. 83 (1985) 166.
[66] R.H. Schultz, P.B. Armentrout, Int. J. Mass Spectrom. Ion. Processes 107 (1991) 29.
[67] W.J. Chesnavich, M.T. Bowers, J. Phys. Chem. 83 (1979) 900.
[68] P.B. Armentrout, Advances in Gas Phase Ion Chemistry, Vol. 1, N.G. Adams, L.M. Babcock (Eds.), JAI, Greenwich, 1992, pp. 83–119.
[69] T. Shimanouchi, Table of Molecular Vibrational Frequencies, Consolidated, Vol. I, National Bureau of Standards, Washington, DC, 1972.
[70] K.M. Ervin, S. Gronert, S.E. Barlow, M.K. Gilles, A.G. Harrison, V.M. Bierbaum, C.H. DePuy, W.C. Lineberger, G.B. Ellison, J. Am. Chem. Soc. 112 (1990) 5750.
[71] M.S. Robinson, M.L. Polak, V.M. Bierbaum, C.H. DePuy, W.C. Lineberger, J. Am. Chem. Soc. 117 (1995) 6766.
[72] G. Gioumousis, D.P. Stevenson, J. Chem. Phys. 29 (1958) 294.
[73] N. Aristov, P.B. Armentrout, J. Am. Chem. Soc. 106 (1984) 4065.
[74] D.M. Rayner, S.A. Mitchell, O.L. Bourne, P.A. Hackett, J. Opt. Soc. Am. B 4 (1987) 900.
[75] C.W. Bauschlicher Jr., S.R. Langhoff, H. Partridge, in Organometallic Ion Chemistry, B.S. Freiser (Ed.), Kluwer, Dordrecht, 1995, pp. 47–87.
[76] D.E. Clemmer, N. Aristov, P.B. Armentrout, J. Phys. Chem. 97 (1993) 544.
[77] M.R. Sievers, L.M. Jarvis, P.B. Armentrout, J. Am. Chem. Soc. 120 (1998) 1891.
[78] C.E. Moore, Atomic Energy Levels, Natl. Stand. Ref. Data Ser., Vol. II, National Bureau of Standards, Washington, DC, 1971, p. 35.
[79] J. Sugar, C. Corliss, J. Phys. Chem. Ref. Data 14 (1985) 1 (Suppl. 2).